ACS Medicinal Chemistry Letters

Letter

Cite This: ACS Med. Chem. Lett. 2018, 9, 746−751

Optimization of 3-Pyrimidin-4-yl-oxazolidin-2-ones as Orally Bioavailable and Brain Penetrant Mutant IDH1 Inhibitors

Qian Zhao,*[,†] James R. Manning,*[,†] James Sutton,[†,§] Abran Costales,[†,∥] Martin Sendzik,[†,‡] Cynthia M. Shafer,[†] Julian R. Levell,[‡,⊥] Gang Liu,[‡] Thomas Caferro,[‡] Young Shin Cho,[‡] Mark Palermo,[‡] Gregg Chenail,[‡] Julia Dooley,[‡] Brian Villalba,[‡] Ali Farsidjani,[‡] Jinyun Chen,[‡] Stephanie Dodd,[‡] Ty Gould,[‡] Guiqing Liang,[‡] Kelly Slocum,[‡] Minying Pu,[‡] Brant Firestone,[‡] Joseph Growney,[‡] Tycho Heimbach,[‡] and Raymond Pagliarini[‡]

[†]Novartis Institutes for BioMedical Research, 5300 Chiron Way, Emeryville, California 94608, United States

[‡]Novartis Institutes for BioMedical Research, 250 Massachusetts Avenue, Cambridge, Massachusetts 02139, United States

Supporting Information

ABSTRACT: Mutant isocitrate dehydrogenase 1 (IDH1) is an attractive therapeutic target for the treatment of various cancers such as AML, glioma, and glioblastoma. We have evaluated 3-pyrimidin-4-yl-oxazolidin-2-ones as mutant IDH1 inhibitors that bind to an allosteric, induced pocket of IDH1^{R132H}. This Letter describes SAR exploration focused on improving both the *in vitro* and *in vivo* metabolic stability of the compounds, leading to the identification of **19** as a potent and selective mutant IDH1 inhibitor that has demonstrated brain penetration and excellent oral bioavailability in rodents. In a preclinical patient-derived IDH1 mutant xenograft tumor model study, **19** efficiently inhibited the production of the biomarker 2-HG.

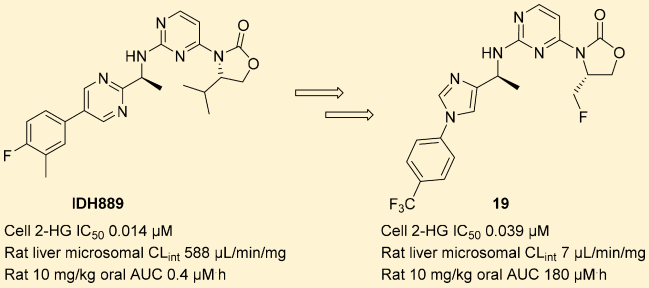

KEYWORDS: *Mutant IDH1, inhibition of 2-HG production, in vivo anticancer activity, brain penetration, clinical candidate*

As an isocitrate dehydrogenase, NADP$^+$-dependent IDH1 catalyzes the oxidative decarboxylation of isocitrate to produce α-ketoglutarate (α-KG) as part of the citric acid cycle in aerobic metabolism,[1−5] while NADP$^+$ is reduced to NADPH.[2−4] Heterozygous mutations in human IDH1 at Arg^{132} (R132*) have been identified in multiple cancer types, including acute myeloid leukemia (AML), glioblastoma, glioma, chondrosarcoma, and cholangiocarcinoma. The gain-of-function mutant loses normal enzymatic function and reduces α-KG to 2-hydroxyglutarate (2-HG), resulting in elevated intracellular levels of this metabolite.[6] 2-HG has been found to inhibit enzymatic function of many α-KG-dependent dioxygenases, including histone and DNA demethylases, causing widespread alterations in histone and DNA methylation which may potentially contribute to tumorigenesis.[7] Recently, a first-in-class inhibitor of mutant IDH1 has shown efficacy against IDH1 mutant glioma and cholangiocarcinoma in clinical studies.[8,9] A number of preclinical studies also provided evidence to support targeting mutant IDH1 tumors with small molecule inhibitors.[10−15]

We recently reported the identification of clinical candidate **IDH305** (**3**) as a brain penetrant, potent, and selective mutant IDH1 inhibitor (Figure 1).[16] A major part of the lead optimization efforts focused on improving intrinsic clearance without compromising physicochemical properties (e.g., solubility). In this Letter, we describe the rational design of fluoromethyl and fluoroethyl (as in **3**) substituted oxazolidinones to enhance metabolic stability.

As reported previously, our hit-to-lead optimization efforts from **1** produced a potent and selective lead compound, **IDH889** (**2**).[17] Oral dosing of **2** in a murine IDH1 mutant tumor xenograft model resulted in robust reduction of tumor-derived 2-HG, a PD biomarker of mutant IDH1^{R132*} activity. However, in addition to low aqueous solubility (39 μM at pH 6.8), **2** also displayed poor rodent PK due to its high *in vivo* clearance (Table 1). This correlated with high *in vitro* intrinsic clearance (CL$_{int}$) across different species (rat/mouse/dog/human 588/143/548/205 μL/min/mg). Thus, improving the CL$_{int}$ was identified as a top priority for the series.

In silico and *in vivo* metabolic studies had identified debenzylation resulting from benzylic oxidation as a major metabolic pathway for **1** (Scheme 1). Common strategies to improve metabolic stability focus on reducing the lipophilicity of the molecule to affect binding to cytochrome P450 proteins (CYPs) and blocking metabolically labile sites.[19]

Our early optimization efforts focused on the exploration of 5-membered heterocyclic aromatic rings on the amine side chain, which were expected to reduce benzylic oxidation[20]

Received: April 16, 2018
Accepted: June 11, 2018
Published: June 11, 2018

DOI: 10.1021/acsmedchemlett.8b00182
ACS Med. Chem. Lett. 2018, 9, 746−751

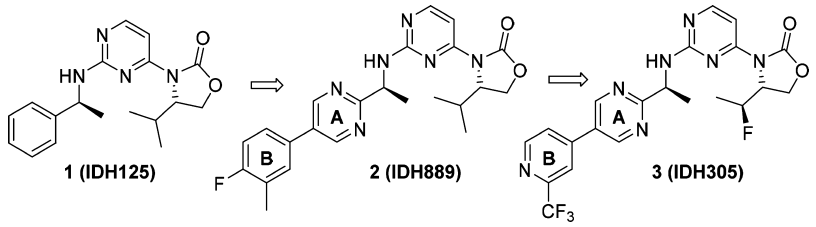

Figure 1. SAR progression from hit-to-lead to clinical candidate.

Table 1. Cellular Potency, *in vitro* CL_{int}, and Rat PK Data of 9, 10, and 2

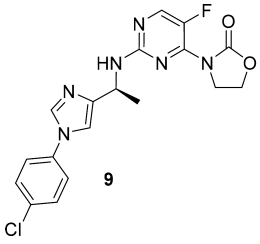

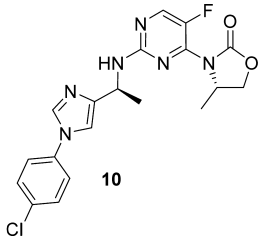

	9	10	2
cellular HCT116-IDH1$^{R132H/+}$ (IC_{50}/μM)	0.56	0.047	0.014
in vitro liver microsomal CL_{int} (μL/min/mg)	34	101	588
in vivo plasma clearance (mL/min/kg)	n.d.[a]	17	41
oral AUC (μM·h)	n.d.	14	0.4
oral bioavailability (%)	n.d.	67	4

[a]Not determined.

Scheme 1. Major Metabolite of 1 in Rat Liver Microsomes

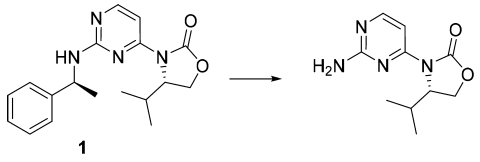

through the inductive effect of the electronegative heteroatoms and reduction of the overall lipophilicity of the molecule. We elected to maintain the isopropyl group on the oxazolidinone ring throughout our initial studies because it enhanced potency relative to compounds lacking this moiety. This is likely due both to its interaction with the hydrophobic protein pocket and, more importantly, its van der Waals contact with the aryl group of the amine side chain. Indeed, both the bound and small molecule X-ray structures of **1** overlay closely, suggesting a prearrangement of the molecule into the active binding conformation that is driven by hydrophobic collapse.[17,18] We believe this ligand preorganization is critical for maintaining mutant IDH1 potency. Additionally, a cocrystal structure of **2**[17] with the homodimer of IDH1^{R132H} showed a hydrogen bond between Ser^{278} and one of the *ortho* nitrogen atoms in the pyrimidine ring. Therefore, in our optimization efforts, at least one hydrogen bond acceptor, either a nitrogen or oxygen atom, was maintained in ring A (Figure 1).

Most of the heterocyclic analogs thus prepared did indeed attenuate the aforementioned benzylic oxidation observed in Met ID studies; however, the rat *in vitro* microsomal CL_{int} remained high. For example, benzylic oxidation of oxadiazole **4** was reduced during incubation with rat liver microsomes (Scheme 2), but the major observed metabolites now resulted from oxazolidinone ring opening and oxidation. The change in the site of metabolism observed with **4** was not predicted by *in silico* modeling, but we were nonetheless encouraged by the reduced benzylic oxidation observed with **4** and *para*-chloro analog **5**, which is more potent and has improved CL_{int}. The tetramethyl substituted analog of **5** (**6**) (Figure 2) was designed

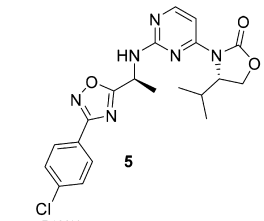

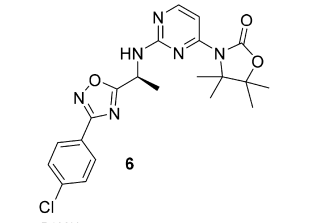

Figure 2. Biochemical potency and rat liver microsomal CL_{int} for **5** and **6**.

and synthesized to block oxazolidinone ring oxidation. Unfortunately, this resulted in a 20-fold loss in potency, and only a slight improvement in CL_{int} was observed.

In parallel to the work on the heteroaromatic analogs, compounds that displayed acceptable CL_{int} (although were insufficiently potent) were evaluated to understand what structural characteristics were important for metabolic stability. For instance, unsubstituted oxazolidinone **7** (Figure 3) had low clearance, while the corresponding isopropyl analog **8** displayed high clearance. It seemed counterintuitive that analogs containing

Scheme 2. Major Metabolites of 4 in Rat Liver Microsomes

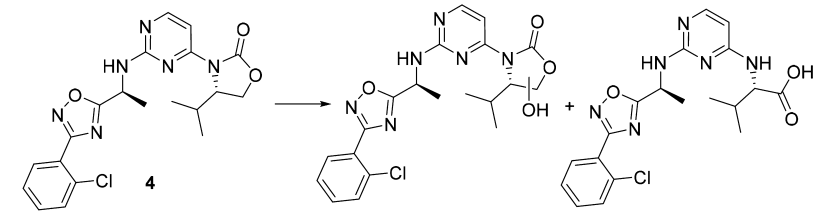

DOI: 10.1021/acsmedchemlett.8b00182
ACS Med. Chem. Lett. 2018, 9, 746−751

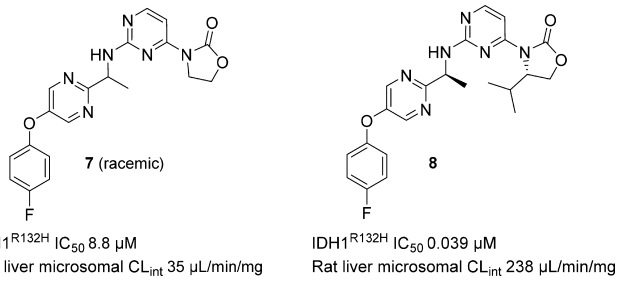

Figure 3. Biochemical potency and rat liver microsomal CL_{int} for **7** and **8**.

sterically encumbered oxazolidinone rings would undergo ring metabolism more readily than their unsubstituted congeners. We hypothesized that the substituents on the oxazolidinone might play a role in CYP recognition and binding that could be important for the metabolic stability of the molecules.

The cocrystal structures of both **IDH125** and **IDH889**[17] showed van der Waals interactions between the isopropyl group and ring A. Thus, the decreased potency of **7** relative to isopropyl analog **8** was not surprising because of the ligand preorganization resulting from the aforementioned hydrophobic collapse.[17] However, the relative importance of the isopropyl group to inducing the hydrophobic collapse was unclear. Therefore, the unsubstituted oxazolidinone was viewed as providing a starting point for building in potency while maintaining good metabolic stability. In addition to high clearance, isopropyl analogs also generally displayed low aqueous solubility and high plasma protein binding across species. Substituents that would reduce lipophilicity as compared to isopropyl would likely improve the overall physicochemical profile of the series and lead to better druglike properties.

Toward this goal, an effort was initiated to evaluate various substituents on both the oxazolidinone and the biaryl amine side chain to identify a suitable combination of metabolic stability and potency. A number of 5,6- and 6,6-membered biaryl analogs were synthesized, and the imidazole analog **9** was identified as a promising lead, with a cellular IC_{50} of 0.5 μM and much improved *in vitro* CL_{int} across species (mouse/rat/human 73/34/59 μL/min/mg). The addition of a methyl group onto the oxazolidinone ring (**10**) increased cellular potency 10-fold, while only moderately increasing the rat CL_{int} (103 μL/min/mg) as compared to **2** and other isopropyl analogs (Table 1). Compound **10** also displayed significantly lower *in vivo* clearance vs **2** (17 vs 41 mL/min/kg) during pharmacokinetic profiling in rat (IV/PO 1/10 mg/kg). This translated to a 35-fold increase in oral AUC and a 17-fold improvement in bioavailability vs **2** at the same oral dosage.

Given these encouraging results, we continued to explore the oxazolidinone substitutions to further improve the stability and potency of the imidazole series. We anticipated that the oxazolidinone SAR would translate beyond the imidazole series described here and that the findings could prove useful for the optimization of the other biaryl series as well. The data summarized in Table 2 highlights both steric and electronic effects of the substituents on cellular IC_{50} and microsomal CL_{int}. Ethyl analog **11** was about 3-fold more potent than methyl analog **10**; however, the CL_{int} of **11** was significantly higher. Introduction of a fluorine atom generated a pair of fluoroethyl diastereomers, **12** and **13**. While both isomers demonstrated a trend toward improved stability over ethyl analog **11**, *S*-isomer **13** was shown to be the more potent diastereomer by 10-fold over **12**.

Table 2. Cellular Potency and CL_{int} in Rat Liver Microsomes

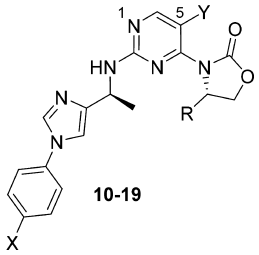

Cmpd	X	Y	R	Cellular HCT116-IDH1$^{R132H/+}$ (IC_{50}/μM)	Rat liver microsomal CL_{int} (μL/min/mg)
10	Cl	F	Me	0.047	103
11	Cl	F	Et	0.013	448
12	Cl	F	(*R*)-1-F-Et	0.24	237
13	Cl	F	(*S*)-1- F-Et	0.022	272
14	Cl	F	F-Me	0.024	28
15	Cl	H	*i*-Pr	0.015	489
16	Cl	H	(*S*)-1- F-Et	0.004	148
17	Cl	H	F-Me	0.030	75
18	CF_2H	H	(*S*)-1- F-Et	0.015	72
19	CF_3	H	F-Me	0.039	7

A significant improvement in stability was obtained with fluoromethyl analog **14** with maintenance of cellular potency.

Throughout our medicinal chemistry campaign, both the 5-fluoro and 5-hydrogen pyrimidine cores had been explored, and the 5-substituent was identified as a handle for the fine-tuning of potency, lipophilicity, and physicochemical properties. As observed in the other biaryl series, isopropyl analog **15** displayed good potency and high CL_{int}. The (*S*)-fluoroethyl analog of **15** (**16**) demonstrated an improvement in potency (4-fold) and stability vs **15**. Once again, lower CL_{int} was observed with fluoromethyl analog **17** relative to **16**. However, unlike with the 5-fluoro pyrimidines (**13**–**14**), the cellular potency dropped over 7-fold from **16** to **17.**

Encouraged by the improvement in CL_{int} with the fluoromethyl and (*S*)-1-fluoroethyl oxazolidinones, we decided to modify the phenyl substitutions of the biaryl amine side chain and identified a number of potent compounds with low to medium CL_{int}, exemplified by **18** and **19**.

Both **18** and **19** demonstrated a good balance of cellular potency, *in vitro* clearance, permeability and aqueous solubility (Table 3). Although **19** was about 2-fold less potent than **18**, its superior microsomal CL_{int} correlated with significantly improved *in vivo* clearance, AUC, and oral bioavailability in rat vs **18**. When rat plasma protein binding data were used to approximate unbound plasma AUC, 10 mg/kg oral dosing of **18** and **19** provided cellular IC_{50} coverage for roughly the same amount of time (Figure SI-1). The AUC brain to plasma ratio of **19** in rat at 10 mg/kg was 0.17, suggesting **19** is brain penetrant. The limited exposure of **18** in rat brain is presumably due to the p-glycoprotein driven efflux mechanism (MDR1-MDCK efflux ratio >9).

Compound **19** was evaluated for specificity against mutant IDH1 relative to wild-type (WT) IDH1 in a biochemical assay measuring consumption (mutant) or production (WT) of NADPH.[21] Compound **19** exhibited over 50- to 100-fold selectivity for mutant IDH1 isoforms vs WT (IDH1^{R132H} IC_{50} 0.021 μM; IDH1^{R132C} IC_{50} 0.045 μM; IDH1^{WT} IC_{50} 2.52 μM).

DOI: 10.1021/acsmedchemlett.8b00182
ACS Med. Chem. Lett. 2018, 9, 746−751

Table 3. Physicochemical Properties and Rodent PK Data for 18 and 19 (IV/PO 1/10 mg/kg for rat and mouse)

	18	19
cellular HCT116-IDH1$^{R132H/+}$ IC_{50} (μM)	0.015	0.039
solubility at pH 6.8 (μM)	422	124
Caco-2 Papp (AB/BA)	21/31	20/24
MDR1-MDCK (AB/BA)	6/57	11/39
plasma protein binding (rat/mouse)	95/92	98/98
in vitro liver microsomal CL_{int} (μL/min/mg) (rat/mouse)	72/63	7.7/11
in vivo plasma clearance (mL/min/kg) (rat/mouse)	20/n.d.[a]	2.6/5
oral AUC (μM·h) (rat/mouse)	15/n.d.	180/172
oral bioavailability (%) (rat/mouse)	82/n.d.	127/149
brain to plasma (total) AUC ratio (rat)	<0.1	0.17

[a]Not determined.

Compound **19** was also profiled in a patient-derived IDH1 mutant HCT116-IDH1$^{R132H/+}$ mechanistic xenograft tumor model in mice to evaluate *in vivo* inhibition of 2-HG production. Compound **19**, dosed orally at 150 mg/kg, inhibited new 2-HG production. Given the high baseline tissue concentration of 2-HG, it takes several hours for it to be cleared from tissues, as observed previously in the pharmacodynamic (PD) study with **2**.[17] Unbound plasma concentration of **19**, approximated from mouse plasma protein binding of 98%, stayed above the HCT116-IDH1$^{R132H/+}$ cellular IC_{50} for 24 h. This resulted in reduction of tumor 2-HG concentration (Figure 4), with

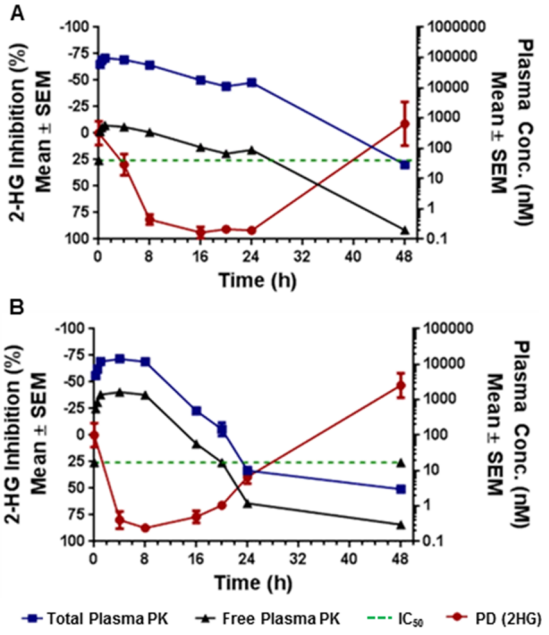

Figure 4. Percent 2-HG inhibition in HCT116-IDH1$^{R132H/+}$ xenograft tumor tissue in correlation with total and calculated unbound plasma concentration following (a) 150 mg/kg dose of **19** and (b) 200 mg/kg dose of **3**.

maximal 2-HG inhibition of over 90% relative to the vehicle-treated tumors at 16−24 h post-treatment. As a comparison, when **3** was dosed orally at 200 mg/kg in the same PK/PD study,[16] 2-HG levels began to rebound after 16 h post-treatment as the free concentration of **3** dropped below the *in vitro* cellular IC_{50}.

The synthesis of **19** is described in Scheme 3. Condensation of (*S*)-2-methylpropane-2-sulfinamide[22] and *tert*-butyl

Scheme 3. Synthesis of 19

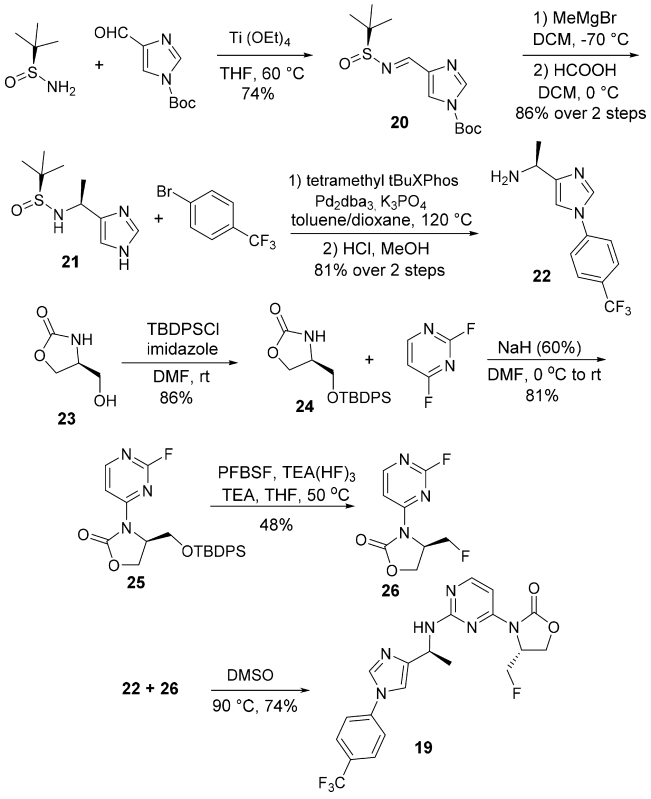

4-formyl-1*H*-imidazole-1-carboxylate provided **20** in 74% yield. The addition of methylmagnesium bromide to *tert*-butanesulfinimine **20**,[23] followed by Boc deprotection gave **21** in 86% yield over two steps. Palladium-catalyzed cross-coupling[24] of **21** with 1-bromo-4-(trifluoromethyl)benzene, followed by removal of the *tert*-butanesulfinyl group, provided amine **22** efficiently in 81% yield over two steps. Silyl protection of (*S*)-4-(hydroxymethyl)oxazolidin-2-one (**23**) produced **24** in 86% yield, and the subsequent S_NAr reaction of **24** with 2,4-difluoropyrimidine afforded compound **25** in 81% yield. The removal of the silyl protecting group and subsequent conversion to fluoromethyl compound **26** was achieved efficiently in one-pot using perfluorobutanesulfonyl fluoride (PFBSF) and triethylamine trihydrofluoride.[25] Coupling of **22** and **26** in DMSO then provided **19** in 74% yield.

Examples can be found in the literature demonstrating that metabolism can be reduced for some molecules when a metabolically labile C−H is replaced by C−F. These include the cholesterol-absorption inhibitor Ezetimibe[26] and the cathepsin K inhibitor Odanacatib[27] for the treatment of osteoporosis. Multiple factors may contribute to the improvement of CL_{int} of the fluoroalkyl-substituted analogs (**12**−**14** and **16**−**19**), including a reduction in potential for oxazolidinone ring oxidation by an inductive effect of the electronegative fluorine atom. Another factor could be the effect of fluorine on molecular lipophilicity. Examples of a hydrogen-to-fluorine substitution decreasing lipophilicity have been reported by Roche scientists.[28] Those compounds contained a common motif whereby an oxygen atom was located either two or three carbons away from a fluorine. The decreased lipophilicity was attributed to the polarization of the oxygen atom by the neighboring fluorine. Interestingly, this structural pattern is also observed in our fluoroalkyl analogs. It is noted that some

DOI: 10.1021/acsmedchemlett.8b00182
ACS Med. Chem. Lett. 2018, 9, 746−751

modifications to the biaryl amine side chain modestly improved CL_{int} of the isopropyl-substituted analogs, but not as substantially as the replacement of the isopropyl group with methyl, fluoromethyl, or fluoroethyl groups. This suggests that the compounds may be recognized differently within the CYP enzyme active site and that the substituents on the oxazolidinone ring can affect the binding of the compounds in the active site.

In conclusion, our optimization of lead compound **2** with a focus on improving *in vitro* CL_{int} led to the discoveries of both the imidazole subseries and fluoroalkyl-substituted oxazolidinones that demonstrated improved metabolic stability. Potent, orally bioavailable and brain-penetrant mutant IDH1 inhibitor **19** effectively inhibited 2-HG production in a preclinical xenograft tumor model. The fluoroalkyl oxazolidinone SAR was also applied to other biaryl series, and a number of compounds with good potency and desirable *in vivo* properties, including the clinical candidate **IDH305**, were subsequently identified.

■ ASSOCIATED CONTENT

Supporting Information

The Supporting Information is available free of charge on the ACS Publications website at DOI: 10.1021/acsmedchemlett.8b00182.

Synthetic procedures, analytical data, assay protocols, PK, PK/PD, and efficacy study protocols and data (PDF)

■ AUTHOR INFORMATION

Corresponding Authors

*E-mail: qianz53705@gmail.com.
*Tel: (510) 879-9429. E-mail: james.manning@novartis.com.

ORCID

James R. Manning: 0000-0002-2111-4723
Julian R. Levell: 0000-0002-6171-3819

Present Addresses

[§](J.S.) Ideaya Biosciences, 280 Utah Avenue, Suite 250, South San Francisco, CA 94080.
[∥](A.C.) Chevron Oronite LLC, 100 Chevron Way, Richmond, CA 94802.
[⊥](J.R.L.) Constellation Pharmaceuticals, 215 First Street, Suite 200, Cambridge, MA 02142.

Notes

The authors declare the following competing financial interest(s): The authors are all current or former employees of Novartis and some own shares in Novartis.

■ ACKNOWLEDGMENTS

The authors would like to thank Dazhi Tang and Weiping Jia for analytical support and Bill Sellers, Karin Briner, Tim Ramsey, Michael Dillon, Juliet Williams, and Travis Stams for project support.

■ REFERENCES

(1) Dimitrov, L.; Hong, C. S.; Yang, C.; Zhuang, Z.; Heiss, J. D. New developments in the pathogenesis and therapeutic targeting of the IDH1 mutation in glioma. *Int. J. Med. Sci.* **2015**, *12* (3), 201−213.

(2) Molenaar, R. J.; Radivoyevitch, T.; Maciejewski, J. P.; van Noorden, C. J. F.; Bleeker, F. E. The driver and passenger effects of isocitrate dehydrogenase 1 and 2 mutations in oncogenesis and survival prolongation. *Biochim. Biophys. Acta, Rev. Cancer* **2014**, *1846* (2), 326−341.

(3) Kim, H.−J.; Fei, X.; Cho, S.−C.; Choi, B. Y.; Ahn, H.−C.; Lee, K.; Seo, S.−Y.; Keum, Y.−S. Discovery of α-mangostin as a novel competitive inhibitor against mutant isocitrate dehydrogenase-1. *Bioorg. Med. Chem. Lett.* **2015**, *25*, 5625−5631.

(4) Guo, C.; Pirozzi, C. J.; Lopez, G. Y.; Yan, H. Isocitrate dehydrogenase mutations in gliomas: mechanisms, biomarkers and therapeutic target. *Curr. Opin. Neurol.* **2011**, *24* (6), 648−652.

(5) Xu, X.; Zhao, J.; Xu, Z.; Peng, B.; Huang, Q.; Arnold, E.; Ding, J. Structures of human cytosolic NADP-dependent isocitrate dehydrogenase reveal a novel self-regulatory mechanism of activity. *J. Biol. Chem.* **2004**, *279*, 33946−33957.

(6) Turkalp, Z.; Karamchandani, J.; Das, S. IDH mutation in glioma: new insights and promises for the future. *JAMA Neurology* **2014**, *71*, 1319−1325.

(7) Liu, X.; Ling, Z. Q. Role of isocitrate dehydrogenase 1/2 (IDH 1/2) gene mutations in human tumors. *Histology and Histopathology* **2015**, *30*, 1155−1160.

(8) Hansen, E.; Quivoron, C.; Straley, K.; Lemieux, R. M.; Popovici-Muller, J.; Sadrzadeh, H.; Fathi, A. T.; Gliser, C.; David, M.; Saada, V.; Micol, J.−B.; Bernard, O.; Dorsch, M.; Yang, H.; Su, M.; Agresta, S.; de Botton, S.; Penard-Lacronique, V.; Yen, K. AG-120, an oral, selective, first-in-class, potent inhibitor of mutant IDH1, reduces intracellular 2HG and induces cellular differentiation in TF-1 R132H cells and primary human IDH1 mutant AML patient samples treated ex vivo. *Blood* **2014**, *124*, 3734.

(9) Mondesir, J.; Willekens, C.; de Botton, S. IDH1 and IDH2 mutations as novel therapeutic targets: current perspectives. *J. Blood Med.* **2016**, *7*, 171−180.

(10) Popovici-Muller, J.; Saunders, J. O.; Salituro, F. G.; Travins, J. M.; Yan, S.; Zhao, F.; Gross, S.; Dang, L.; Yen, K. E.; Yang, H.; Straley, K. S.; Jin, S.; Kunii, K.; Fantin, V. R.; Zhang, S.; Pan, Q.; Shi, D.; Biller, S. A.; Su, S. M. Discovery of the first potent inhibitors of mutant IDH1 that lower tumor 2-HG in vivo. *ACS Med. Chem. Lett.* **2012**, *3*, 850−855.

(11) Liu, Z.; Yao, Y.; Kogiso, M.; Zheng, B.; Deng, L.; Qiu, J. J.; Dong, S.; Lv, H.; Gallo, J. M.; Li, X.−N.; Song, Y. Inhibition of cancer-associated mutant isocitrate dehydrogenases: synthesis, structure−activity relationship, and selective antitumor activity. *J. Med. Chem.* **2014**, *57*, 8307−8318.

(12) Brooks, E.; Wu, X.; Hanel, A.; Nguyen, S.; Wang, J.; Zhang, J. H.; Harrison, A.; Zhang, W. Identification and characterization of small-molecule inhibitors of the R132H/R132H mutant isocitrate dehydrogenase 1 homodimer and R132H/wild-type heterodimer. *J. Biomol. Screening* **2014**, *19*, 1193−1200.

(13) Deng, G.; Shen, J.; Yin, M.; McManus, J.; Mathieu, M.; Gee, P.; He, T.; Shi, C.; Bedel, O.; McLean, L. R.; Le-Strat, F.; Zhang, Y.; Marquette, J.−P.; Gao, Q.; Zhang, B.; Rak, A.; Hoffmann, D.; Rooney, E.; Vassort, A.; Englaro, W.; Li, Y.; Patel, V.; Adrian, F.; Gross, S.; Wiederschain, D.; Cheng, H.; Licht, S. Selective inhibition of mutant isocitrate dehydrogenase 1 (IDH1) via disruption of a metal binding network by an allosteric small molecule. *J. Biol. Chem.* **2015**, *290*, 762−774.

(14) Rohle, D.; Popovici-Muller, J.; Palaskas, N.; Turcan, S.; Grommes, C.; Campos, C.; Tsoi, J.; Clark, O.; Oldrini, B.; Komisopoulou, E.; Kunii, K.; Pedraza, A.; Schalm, S.; Silverman, L.; Miller, A.; Wang, F.; Yang, H.; Chen, Y.; Kernytsky, A.; Rosenblum, M. K.; Liu, W.; Biller, S. A.; Su, S. M.; Brennan, C. W.; Chan, T. A.; Graeber, T. G.; Yen, K. E.; Mellinghoff, I. K. An inhibitor of mutant IDH1 delays growth and promotes differentiation of glioma cells. *Science* **2013**, *340*, 626−630.

(15) Zheng, B.; Yao, Y.; Liu, Z.; Deng, L.; Anglin, J. L.; Jiang, H.; Prasad, B. V. V.; Song, Y. Crystallographic investigation and selective inhibition of mutant isocitrate dehydrogenase. *ACS Med. Chem. Lett.* **2013**, *4*, 542−546.

(16) Cho, Y. S.; Levell, J. R.; Liu, G.; Caferro, T.; Sutton, J.; Shafer, C. M.; Costales, A.; Manning, J. R.; Zhao, Q.; Sendzik, M.; Shultz, M.; Chenail, G.; Dooley, J.; Villalba, B.; Farsidjani, A.; Chen, J.; Kulathila, R.; Xie, X.; Dodd, S.; Gould, T.; Liang, G.; Heimbach, T.; Slocum, K.; Firestone, B.; Pu, M.; Pagliarini, R.; Growney, J. D. Discovery and evaluation of clinical candidate IDH305, a brain penetrant mutant IDH1 inhibitor. *ACS Med. Chem. Lett.* **2017**, *8*, 1116−1121.

DOI: 10.1021/acsmedchemlett.8b00182
ACS Med. Chem. Lett. 2018, 9, 746−751

(17) Levell, J. R.; Caferro, T.; Chenail, G.; Dix, I.; Dooley, J.; Firestone, B.; Fortin, P. D.; Giraldes, J.; Gould, T.; Growney, J. D.; Jones, M. D.; Kulathila, R.; Lin, F.; Liu, G.; Mueller, A.; van der Plas, S.; Slocum, K.; Smith, T.; Terranova, R.; Touré, B. B.; Tyagi, V.; Wagner, T.; Xie, X.; Xu, M.; Yang, F. S.; Zhou, L. X.; Pagliarini, R.; Cho, Y. S. Optimization of 3-pyrimidin-4-yl-oxazolidin-2-ones as allosteric and mutant specific inhibitors of IDH1. *ACS Med. Chem. Lett.* **2017**, *8*, 151−156.
(18) Xie, X.; Baird, D.; Bowen, K.; Capka, V.; Chen, J.; Chenail, G.; Cho, Y. S.; Dooley, J.; Farsidjani, A.; Fortin, P.; Kohls, D.; Kulathila, R.; Lin, F.; McKay, D.; Rodrigues, L.; Sage, D.; Touré, B. B.; van der Plas, S.; Wright, K.; Xu, M.; Yin, H.; Levell, J.; Pagliarini, R. A. Allosteric mutant IDH1 inhibitors reveal mechanisms for IDH1 mutant and isoform selectivity. *Structure* **2017**, *25*, 506−513.
(19) Nassar, A.−E. F.; Kamel, A. M.; Clarimont, C. Improving the decision-making process in the structural modification of drug candidates: enhancing metabolic stability. *Drug Discovery Today* **2004**, *9*, 1020−1028.
(20) Ioannidis, S.; Lamb, M. L.; Wang, T.; Almeida, L.; Block, M. H.; Davies, A. M.; Peng, B.; Su, M.; Zhang, H.−J.; Hoffmann, E.; Rivard, C.; Green, I.; Howard, T.; Pollard, H.; Read, J.; Alimzhanov, M.; Bebernitz, G.; Bell, K.; Ye, M.; Huszar, D.; Zinda, M. Discovery of 5-Chloro-N^2-[(1*S*)-1-(5-fluoropyrimidin-2-yl)ethyl]-N^4-(5-methyl-1*H*-pyrazol-3-yl)pyrimidine-2,4-diamine (AZD1480) as a Novel Inhibitor of the Jak/Stat Pathway. *J. Med. Chem.* **2011**, *54*, 262−276.
(21) Gao, H.; Korn, J. M.; Ferretti, S.; Monahan, J. E.; Wang, Y.; Singh, M.; Zhang, C.; Schnell, C.; Yang, G.; Zhang, Y.; Balbin, O. A.; Barbe, S.; Cai, H.; Casey, F.; Chatterjee, S.; Chiang, D. Y.; Chuai, S.; Cogan, S. M.; Collins, S. D.; Dammassa, E.; Ebel, N.; Embry, M.; Green, J.; Kauffmann, A.; Kowal, C.; Leary, R. J.; Lehar, J.; Liang, Y.; Loo, A.; Lorenzana, E.; McDonald, E. R., III; McLaughlin, M. E.; Merkin, J.; Meyer, R.; Naylor, T. L.; Patawaran, M.; Reddy, A.; Röelli, C.; Ruddy, D. A.; Salangsang, F.; Santacroce, F.; Singh, A. P.; Tang, Y.; Tinetto, W.; Tobler, S.; Velazquez, R.; Venkatesan, K.; Von Arx, F.; Wang, H. Q.; Wang, Z.; Wiesmann, M.; Wyss, D.; Xu, F.; Bitter, H.; Atadja, P.; Lees, E.; Hofmann, F.; Li, E.; Keen, N.; Cozens, R.; Jensen, M. R.; Pryer, N. K.; Williams, J. A.; Sellers, W. R. High-throughput screening using patient-derived tumor xenografts to predict clinical trial drug response. *Nat. Med.* **2015**, *21*, 1318−1325.
(22) Collados, J. F.; Toledano, E.; Guijarro, D.; Yus, M. Microwave-assisted solvent-free synthesis of enantiomerically pure N-(tert-butylsulfinyl)imines. *J. Org. Chem.* **2012**, *77*, 5744−5750.
(23) Liu, G.; Cogan, D. A.; Ellman, J. A. Catalytic asymmetric synthesis of tert-butanesulfinamide. Application to the asymmetric synthesis of amines. *J. Am. Chem. Soc.* **1997**, *119*, 9913−9914.
(24) Ueda, S.; Ali, S.; Fors, B. P.; Buchwald, S. L. Me_3(OMe)-tBuXPhos: A surrogate ligand for Me_4tBuXPhos in palladium-catalyzed C−N and C−O bond-forming reactions. *J. Org. Chem.* **2012**, *77*, 2543−2547.
(25) Yin, J.; Zarkowsky, D. S.; Thomas, D. W.; Zhao, M. M.; Huffman, M. A. Direct and convenient conversion of alcohols to fluorides. *Org. Lett.* **2004**, *6*, 1465−1468.
(26) Van Heek, M.; France, C. F.; Compton, D. S.; Mcleod, R. L.; Yumibe, N. P.; Alton, K. B.; Sybertz, E. J.; Davis, H. R., Jr In vivo metabolism-based discovery of a potent cholesterol absorption inhibitor, SCH58235, in the rat and rhesus monkey through the identification of the active metabolites of SCH48461. *J. Pharmacol. Exp. Ther.* **1997**, *283*, 157−163.
(27) Gauthier, J. Y.; Chauret, N.; Cromlish, W.; Desmarais, S.; Duong, L. T.; Falgueyret, J.−P.; Kimmel, D. B.; Lamontagne, S.; Léger, S.; LeRiche, T.; Li, C. S.; Massé, F.; McKay, D. J.; Nicoll-Griffith, D. A.; Oballa, R. M.; Palmer, J. T.; Percival, M. D.; Riendeau, D.; Robichaud, J.; Rodan, G. A.; Rodan, S. B.; Seto, C.; Thérien, M.; Truong, V.−L.; Venuti, M. C.; Wesolowski, G.; Young, R. N.; Zamboni, R.; Black, W. C. The discovery of odanacatib (MK-0822), a selective inhibitor of cathepsin K. *Bioorg. Med. Chem. Lett.* **2008**, *18*, 923−928.
(28) Böhm, H.−J.; Banner, D.; Bendels, S.; Kansy, M.; Kuhn, B.; Müller, K.; Obst-Sander, U.; Stahl, M. Fluorine in medicinal chemistry. *ChemBioChem* **2004**, *5*, 637−643.

DOI: 10.1021/acsmedchemlett.8b00182
ACS Med. Chem. Lett. 2018, 9, 746−751